

Incremental Relaying for Power Line Communication: Performance Analysis and Power Allocation

Ankit Dubey, *Member, IEEE*, Chinmoy Kundu, *Member, IEEE*, Telex M. N. Ngatched, *Senior Member, IEEE*, Octavia A. Dobre, *Senior Member, IEEE*, and Ranjan K. Mallik, *Fellow, IEEE*

Abstract

In this paper, incremental decode-and-forward (IDF) and incremental selective decode-and-forward (ISDF) relaying are proposed to improve the spectral efficiency of power line communication. Contrary to the traditional decode-and-forward (DF) relaying, IDF and ISDF strategies utilize the relay only if the direct link ceases to attain a certain information rate, thereby improving the spectral efficiency. The path gain through the power line is assumed to be log-normally distributed with high distance-dependent attenuation and the additive noise is from a Bernoulli-Gaussian process. Closed-form expressions for the outage probability, and approximate closed-form expressions for the end-to-end average channel capacity and the average bit error rate for binary phase-shift keying are derived. Furthermore, a closed-form expression for the fraction of times the relay is in use is derived as a measure of the spectral efficiency. Comparative analysis of IDF and ISDF with traditional DF relaying is presented. It is shown that IDF is a specific case of ISDF and can obtain optimal spectral efficiency without compromising the outage performance. By employing power allocation to minimize the outage probability, it is realized that the power should be allocated in accordance with the inter-node distances and channel parameters.

Index Terms

Bernoulli-Gaussian impulsive noise, bit error rate (BER), incremental decode-and-forward (IDF), incremental selective decode-and-forward (ISDF), log-normal fading, power allocation, power line communication.

Manuscript received June 13, 2018; revised October 26, 2018; accepted October 28, 2018. This work was supported in part by the Department of Science and Technology (DST), Govt. of India (Ref. No. TMD/CERI/BEE/2016/059(G)), the Science and Engineering Research Board (SERB), Govt. of India through its Early Career Research (ECR) Award (Ref. No. ECR/2016/001377), Royal Society-SERB Newton International Fellowship under Grant NF151345, and Natural Science and Engineering Research Council of Canada (NSERC) through its Discovery program. (Corresponding author: Octavia Dobre.)

Ankit Dubey is with the Department of ECE, National Institute of Technology Goa, Farmagudi, Ponda, Goa 403401, India, e-mail: ankit.dubey@nitgoa.ac.in.

Chinmoy Kundu is with the School of Electronics, Electrical Engineering and Computer Science, Queen's University Belfast, U.K., e-mail: c.kundu@qub.ac.uk.

Telex M. N. Ngatched and Octavia A. Dobre are with the Faculty of Engineering and Applied Science, Memorial University, Canada, e-mail: tngatched@grenfell.mun.ca, odobre@mun.ca.

Ranjan K. Mallik is with the Department of Electrical Engineering, Indian Institute of Technology Delhi, New Delhi 110016, India, e-mail: rkmallik@ee.iitd.ernet.in.

I. INTRODUCTION

Power line communication (PLC) is a key solution that is driving Internet-of-Things (IoT) based smart grid, home automation, and many such other concepts. Being a retrofit technology, PLC does not need extra communication links to be deployed, unlike optical and other traditional wireline communication systems [1]. Furthermore, due to the omnipresence of power lines, unlike wireless system, PLC has greater device-to-device (appliance-to-appliance) connectivity that makes PLC one of the suitable candidates for IoT [2], [3].

Implementation cost and resource complexity for a PLC system is much lower when compared to other wireline communication systems, but it has its own hurdles. A power line is designed to carry high power alternating current signals at very low frequency (around 45 to 65 Hz); on the contrary, in PLC systems, data symbols are transmitted with very small signal power over a high frequency carrier, and hence, are subjected to high signal attenuation [1]. Additionally, due to the mesh structure of the power distribution, the communication signal transmitted using power line reaches the receiver through multiple paths, which causes signal fading. In many scenarios, fading in the PLC channel is shown to follow the log-normal distribution [4]–[6]. Furthermore, due to frequent load switching and integration of new home and industry appliances like light emitting diode lamps, stepper motors, air conditioners, induction plates, etc., data symbols transmitted through power lines suffer from impulsive noise [1], [7].

As in wireless communication, reliability of data transmission in PLC systems can also be enhanced with the aid of relays [8], [9]. Similar to a wireless system, the relay in a PLC system can be a dedicated or a cooperative node and can act in amplify-and-forward (AF) or decode-and-forward (DF) mode. A study on cooperative coding for narrowband PLC has been presented in [8]. A distributed space-time coding for multi-hop transmission has been introduced in [9]. A bound on channel capacity is derived using AF relays in [10]. An opportunistic routing for smart grid with PLC access networks is presented in [11]. Recently, the average bit error rate (BER) and outage analyses using DF and AF relays have been studied in [12] and [13], respectively, where the possibility of direct transmission has been overruled. Furthermore, to address the relay selection problem for dual-hop transmission, a class of machine learning schemes has been proposed in [14]. Recently, DF energy-harvesting based relaying has been proposed for PLC and the issue of energy-efficiency has also been discussed in [15], [16]. Very recently, the ergodic achievable data rate of the so-called incomplete hybrid power line-wireless single-relay channel model has been studied in [17].

In the above literature, the relays are generally DF or AF type with half-duplex transmission capability, which requires two time slots to complete the information transmission from source to destination [18], [19]. It is possible to improve the system spectral efficiency by using a relaying technique referred to as incremental relaying [19]. Incremental relaying exploits feedback from the destination to decide whether or not relaying is necessary for retransmission of the source message. In incremental relaying, the relay is used only if the direct transmission from source to destination fails to achieve a required information rate. In combination with DF relays, incremental relaying can be applied through the following two schemes: i) incremental DF (IDF) or ii) incremental selective DF (ISDF). In the IDF technique, relaying takes place every time the direct transmission fails. On the other hand,

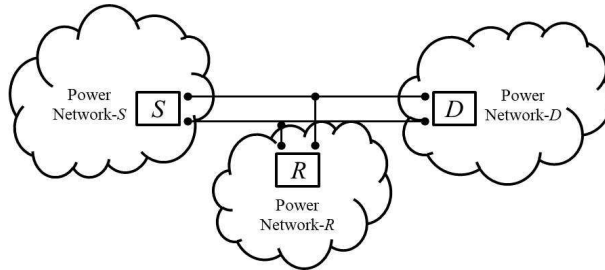


Fig. 1: Relay based PLC system.

in the ISDF strategy, the relay is utilized when the direct transmission fails and the source-to-relay link achieves a required information rate. Though incremental relaying has been investigated in wireless systems (see [20]–[22] and the references therein), to the best of our knowledge, it has not been studied yet in depth in PLC systems. Very recently, work reported in [24] has introduced incremental selective relaying for the PLC for the first time. However, contributions are limited to only independent and identically distributed (i.i.d.) channels. Moreover, the analysis is limited to the outage probability and the average BER.

In this paper, the use of incremental relaying techniques, IDF and ISDF, is proposed and investigated to enhance the spectral efficiency of PLC systems. It is assumed that the PLC channel suffers from log-normal fading with high distance-dependent attenuation, along with Bernoulli-Gaussian impulsive noise. Closed-form expression for the outage probability and approximate closed-form expressions for the end-to-end average channel capacity and average BER are derived and compared with traditional DF relaying. The fraction of times the relay is in use is also investigated as a measure of the spectral efficiency. Furthermore, a technique to minimize the outage probability with appropriate power allocated to the source and relay is investigated.

The rest of the paper is organized as follows. Section II describes the system model, while an approximate closed-form expression for the end-to-end average channel capacity, a closed-form expression for the outage probability, and an approximate closed-form expression for the average BER are derived in Sections III, IV, and V, respectively. Later, a closed-form expression for the fraction of times the relay is in use is derived in Section VI. The power allocation problem is investigated in Section VII. Section VIII presents numerical and simulation results, whereas Section IX provides concluding remarks.

Notation: $\mathbb{E}[\cdot]$ denotes the expectation operator, $\Pr(\cdot)$ denotes the probability of an event, $P_e(\cdot)$ denotes the probability of bit error, $F_X(\cdot)$ represents the cumulative distribution function (CDF) of the random variable (r.v.) X , and $f_X(\cdot)$ is the corresponding probability density function (PDF).

II. SYSTEM MODEL

Consider a PLC system, as shown in Fig. 1, wherein the source, S , communicates with the destination, D , over a power cable. A half-duplex DF relay, R , is placed in between S and D to assist S forward its symbols. A link between any two nodes is denoted by i , where $i \in \{0, 1, 2\}$, and 0, 1, and 2 denote the SD , SR , and

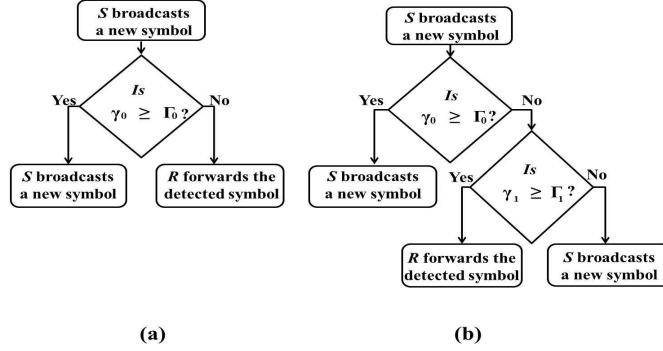


Fig. 2: Relaying strategies: (a) IDF and (b) ISDF.

RD links, respectively. S broadcasts a symbol with transmit power P_S in the first time slot, which is received by D and R . Two different relaying strategies, IDF and ISDF, are studied. In the IDF strategy, R transmits the decoded symbol in the second time slot whenever the direct transmission (SD link) fails to attain a predefined rate threshold, R_{th} , or equivalently when the instantaneous signal-to-noise ratio (SNR) of the SD link, γ_0 , falls below a predefined threshold Γ_0 . On the contrary, the ISDF strategy sets a predefined rate threshold or equivalently an SNR threshold, Γ_1 , at R to restrict the transmission below a certain rate requirement through the SR link, i.e., when the instantaneous SNR of the SR link, γ_1 , falls below Γ_1 . Fig. 2 illustrates the comparison flowchart. In both cases, the relayed link is only used if the direct transmission rate fails to attain R_{th} to improve spectral efficiency. Moreover, in both strategies, S broadcasts a new symbol immediately after the preceding symbol if R does not participate; otherwise, it waits until the relay completes forwarding the previous symbol.

A. Channel Model and Received Power

The received symbol, y_i , through the i th link is given by

$$y_i = \sqrt{P_i} h_i s + z_i, \quad (1)$$

where P_i is the received power, h_i is the channel gain of the i th link, z_i is the additive noise sample at the receiver, and s is the unit power transmitted symbol. Since all nodes have non-identical local power networks (nearby loads) attached to them, as shown in Fig. 1, the PLC channels among different nodes can be considered to be independent but non-identical [4]–[6]. Thus, the channel gain multiplier, h_i , is modeled as an independently distributed log-normal r.v. with PDF

$$f_{h_i}(x) = \frac{1}{x\sqrt{2\pi\xi_i^2}} \exp\left(-\frac{1}{2}\left(\frac{\ln x - \Xi_i}{\xi_i}\right)^2\right), \quad x \geq 0, \quad (2)$$

where the parameters Ξ_i and ξ_i are the mean and the standard deviation of the normal r.v. $\ln(h_i)$, respectively. The ℓ th moment of h_i is given as [23]

$$\mathbb{E}[h_i^\ell] = \exp\left(\ell\Xi_i + \frac{\ell^2\xi_i^2}{2}\right). \quad (3)$$

We assume unit energy of the channel gain, i.e., $\mathbb{E}[h_i^2] = 1$. According to (3), this implies $\Xi_i = -\xi_i^2$.

The received power, P_i , depends on the transmit power, the length of the power cable, and the path loss. The total transmit power, P_T , is divided among S and R with fractions p_f and $(1-p_f)$, respectively, where $0 < p_f < 1$. Thus, the transmit powers of S and R can be expressed as

$$P_S = p_f P_T, P_R = (1 - p_f) P_T. \quad (4)$$

The length of the power cable from S to D , S to R , and R to D are d_0 , d_1 , and d_2 , respectively. The distances d_1 and d_2 can be expressed as

$$d_1 = d_f d_0, d_2 = (1 - d_f) d_0, \quad (5)$$

where $0 < d_f < 1$. The dB equivalent of the received power through the SD , P_0 , can be expressed as

$$P_0(\text{dB}) = P_S(\text{dB}) - d_0(\text{km}) \times P_L(\text{dB/km}), \quad (6)$$

where $P_L(\text{dB/km})$ denotes the path loss factor per unit length. The dB equivalent of P_1 and P_2 can also be similarly expressed.

B. Noise Model and SNR

The symbols transmitted through power lines suffer from impulsive noise [1], [7]. Among several proposed noisy channel model, the Bernoulli-Gaussian model [25] is the mostly used [12], [13]. The model consists of a mixture of two Gaussian processes with different power spectral densities and average occurrence of the impulsive noise with Bernoulli process. According to this noise model, the additive noise sample, z_i , can be written as

$$z_i = w_i + b_i l_i, \quad (7)$$

where w_i and l_i represent background and impulsive noise samples, respectively, and b_i is a Bernoulli r.v. which equals 1 with probability Λ and 0 with probability $(1 - \Lambda)$. The samples w_i and l_i are taken from the Gaussian distribution with mean zero and variances σ_w^2 and σ_l^2 , respectively. Furthermore, w_i , l_i , and b_i are considered to be independent as background and impulsive noise have different origins [26]. Therefore, the noise samples, z_i , are i.i.d. r.v.s, with PDF [25]

$$f_{z_i}(x) = \sum_{j=1}^2 \frac{\Lambda_j}{\sqrt{2\pi\epsilon_j^2}} \exp\left(\frac{-x^2}{2\epsilon_j^2}\right), \quad (8)$$

where

$$\Lambda_1 = 1 - \Lambda, \quad \Lambda_2 = \Lambda, \quad \epsilon_1^2 = \sigma_w^2, \quad \epsilon_2^2 = \sigma_w^2 + \sigma_l^2. \quad (9)$$

The average noise power, N_0 , for all i is given as

$$N_0 = \mathbb{E}[z_i^2] = \mathbb{E}[w_i^2] + \mathbb{E}[b_i^2] \mathbb{E}[l_i^2] = \sigma_w^2(1 + \Lambda \eta), \quad (10)$$

where $\eta = \sigma_l^2/\sigma_w^2$ represents the power ratio of impulsive-to-background noise.

As the channel gain, h_i , is log-normally distributed, the corresponding instantaneous SNR, $\gamma_i = \frac{P_i h_i^2}{N_0}$, is also log-normally distributed with parameters

$$\mu_i = 2\Xi_i + \ln(P_i/N_0), \quad \sigma_i = 2\xi_i. \quad (11)$$

The CDF of γ_i is therefore given by

$$F_{\gamma_i}(x) = \Pr[\gamma_i \leq x] = 1 - Q\left(\frac{\ln x - \mu_i}{\sigma_i}\right), \quad x \geq 0, \quad (12)$$

where $Q(\cdot)$ denotes the Gaussian Q -function defined as [30]

$$Q(x) \triangleq \int_x^\infty \frac{1}{\sqrt{2\pi}} \exp\left(-\frac{t^2}{2}\right) dt. \quad (13)$$

C. SNR Threshold for Rate Requirement

The instantaneous channel capacity of the i th link corrupted by Bernoulli-Gaussian impulsive noise is expressed as [31]

$$\mathcal{C}(\gamma_i) = \sum_{j=1}^2 \Lambda_j \log_2(1 + \tau_j \gamma_i), \quad (14)$$

where τ_1 and τ_2 are given by

$$\tau_1 = \frac{1 + \Lambda\eta}{2}, \quad \tau_2 = \frac{1 + \Lambda\eta}{2(1 + \eta)}. \quad (15)$$

At high SNR (P_i/N_0), i.e., when $\tau_j \gamma_i \gg 1$, the instantaneous channel capacity can be simplified as [12]

$$\mathcal{C}(\gamma_i) \approx \frac{1}{\ln(2)} \left(\sum_{j=1}^2 \ln(\tau_j^{\Lambda_j}) + \ln(\gamma_i) \right). \quad (16)$$

To maintain R_{th} at D through the direct link, a specific SNR threshold, Γ_0 , must be maintained; this can be evaluated from (16) as

$$\Gamma_0 = \tau_1^{-\Lambda_1} \tau_2^{-\Lambda_2} 2^{R_{th}}. \quad (17)$$

To maintain R_{th} at D through the relayed link, the end-to-end SNR threshold in relayed link, Γ_{th} , should be twice the rate of the direct link due to the half-duplex relaying

$$\Gamma_{th} = \tau_1^{-\Lambda_1} \tau_2^{-\Lambda_2} 2^{2R_{th}}. \quad (18)$$

If the relay is in operation, information takes two time slots to reach the destination. On the contrary, direct transmission only takes one time slot. The SNR threshold at the destination and relay determines how frequently the relay will be used, and thereby, the latency associated with it. Thus, in order to improve the spectral efficiency by reducing the relay usage, we selectively decode-and-forward the signal at the relay by setting an SNR threshold Γ_1 for the ISDF scheme. In a practical set up, the value of Γ_1 can be selected based on various factors like instantaneous battery level, minimum required rate, latency, and relay placement. In this work, we select a variable Γ_1 and evaluate the system performance.

III. AVERAGE CHANNEL CAPACITY

In this section, we derive the end-to-end average channel capacity for the relaying strategies. The average channel capacity is derived using the capacity definition provided in the high SNR in (16) to alleviate the difficulty in dealing with (14) to find a closed-form.

A. IDF

While employing IDF, the end-to-end average channel capacity can be calculated as the sum of average capacities of direct and relayed transmissions. The average capacity of the direct transmission is calculated when the SD link SNR meets the threshold requirement and in relayed transmission, it is calculated when the SD link does not meet the threshold. Thus, the average capacity of the system can be obtained using the laws of total probability as

$$\mathcal{C}_{IDF} = \mathbb{E}[\mathcal{C}(\gamma_0 | \gamma_0 > \Gamma_0)] + \frac{1}{2} \Pr[\gamma_0 < \Gamma_0] \mathbb{E}[\mathcal{C}(\gamma_m)], \quad (19)$$

where $\gamma_m = \min\{\gamma_1, \gamma_2\}$ and the factor $1/2$ in the second term comes from half-duplex relaying. Since γ_1 and γ_2 are independent, the PDF of γ_m can be expressed as

$$\begin{aligned} f_{\gamma_m}(x) = & Q\left(\frac{\ln x - \mu_2}{\sigma_2}\right) \frac{1}{x\sqrt{2\pi\sigma_1^2}} \exp\left(-\frac{1}{2}\left(\frac{\ln x - \mu_1}{\sigma_1}\right)^2\right) \\ & + Q\left(\frac{\ln x - \mu_1}{\sigma_1}\right) \frac{1}{x\sqrt{2\pi\sigma_2^2}} \exp\left(-\frac{1}{2}\left(\frac{\ln x - \mu_2}{\sigma_2}\right)^2\right). \end{aligned} \quad (20)$$

From (19), (20), and (16), the end-to-end average channel capacity, for high SNR, can be expressed in closed-form as

$$\begin{aligned} \mathcal{C}_{IDF} = & \frac{1}{\ln(2)} \left\{ \left(\sum_{j=1}^2 \ln(\tau_j^{\Lambda_j} + \mu_0) \right) Q\left(\frac{\ln \Gamma_0 - \mu_0}{\sigma_0}\right) \right. \\ & \left. + \frac{\sigma_0}{\sqrt{2\pi}} \exp\left(-\frac{1}{2}\left(\frac{\ln \Gamma_0 - \mu_0}{\sigma_0}\right)^2\right) \right\} \end{aligned}$$

$$\begin{aligned}
& + \frac{1}{2} \left(1 - Q \left(\frac{\ln \Gamma_0 - \mu_0}{\sigma_0} \right) \right) \left\{ \left(\sum_{j=1}^2 \ln(\tau_j^{\Lambda_j}) \right) \right. \\
& + \mu_1 Q \left(\frac{\mu_1 - \mu_2}{\sqrt{\sigma_1^2 + \sigma_2^2}} \right) - \frac{\sigma_1^2}{\sqrt{2\pi(\sigma_1^2 + \sigma_2^2)}} \\
& \times \exp \left(-\frac{1}{2} \left(\frac{\mu_1 - \mu_2}{\sqrt{\sigma_1^2 + \sigma_2^2}} \right)^2 \right) + \mu_2 Q \left(\frac{\mu_2 - \mu_1}{\sqrt{\sigma_2^2 + \sigma_1^2}} \right) \\
& \left. - \frac{\sigma_2^2}{\sqrt{\sigma_2^2 + \sigma_1^2}} \frac{1}{\sqrt{2\pi}} \exp \left(-\frac{1}{2} \left(\frac{\mu_2 - \mu_1}{\sqrt{\sigma_2^2 + \sigma_1^2}} \right)^2 \right) \right\}. \tag{21}
\end{aligned}$$

$$\begin{aligned}
S_n &= \frac{\Omega_n \sigma_2}{\sqrt{\Omega_n^2 \sigma_1^2 + 2\sigma_2^2}}, T_n = \frac{\Omega_n \sigma_1}{\sqrt{\Omega_n^2 \sigma_2^2 + 2\sigma_1^2}}, E_n = \frac{\Omega_n \sigma_1 (\mu_2 - \mu_1) + 2\Psi_n \sigma_2^2}{\Omega_n^2 \sigma_1^2 + 2\sigma_2^2}, F_n = \frac{\Omega_n \sigma_2 (\mu_1 - \mu_2) + 2\Psi_n \sigma_1^2}{\Omega_n^2 \sigma_2^2 + 2\sigma_1^2}, \\
G_n &= S_n \Phi_n \exp \left(-\frac{1}{2} \left(\left(\frac{\mu_2 - \mu_1}{\sigma_2} \right)^2 + 2 \left(\frac{\Psi_n}{\Omega_n} \right)^2 - \left(\frac{\Omega_n^2 \sigma_1 (\mu_2 - \mu_1) + 2\Psi_n \sigma_2^2}{\Omega_n \sigma_2 \sqrt{\Omega_n^2 \sigma_1^2 + 2\sigma_2^2}} \right)^2 \right) \right), \\
H_n &= T_n \Phi_n \exp \left(-\frac{1}{2} \left(\left(\frac{\mu_1 - \mu_2}{\sigma_1} \right)^2 + 2 \left(\frac{\Psi_n}{\Omega_n} \right)^2 - \left(\frac{\Omega_n^2 \sigma_2 (\mu_1 - \mu_2) + 2\Psi_n \sigma_1^2}{\Omega_n \sigma_1 \sqrt{\Omega_n^2 \sigma_2^2 + 2\sigma_1^2}} \right)^2 \right) \right). \tag{25}
\end{aligned}$$

$$I_4 = \mu_0 Q \left(\frac{\ln(\Gamma_0) - \mu_0}{\sigma_0} \right) + \sigma_0^2 \left(\frac{1}{\sqrt{2\pi\sigma_0^2}} \exp \left(-\frac{1}{2} \left(\frac{\ln(\Gamma_0) - \mu_0}{\sigma_0} \right)^2 \right) \right), \tag{27}$$

$$I_5 = \mu_0 \left(1 - Q \left(\frac{\ln(\Gamma_0) - \mu_0}{\sigma_0} \right) \right) + \sigma_0^2 \left(\frac{-1}{\sqrt{2\pi\sigma_0^2}} \exp \left(-\frac{1}{2} \left(\frac{\ln(\Gamma_0) - \mu_0}{\sigma_0} \right)^2 \right) \right), \tag{28}$$

$$\begin{aligned}
I_6 &= Q \left(\frac{\ln(\Gamma_1) - \mu_1}{\sigma_1} \right) \left\{ \mu_2 \left(1 - Q \left(\frac{\ln(\Gamma_1) - \mu_2}{\sigma_2} \right) \right) + \sigma_2^2 \left(\frac{-1}{\sqrt{2\pi\sigma_2^2}} \exp \left(-\frac{1}{2} \left(\frac{\ln(\Gamma_1) - \mu_2}{\sigma_2} \right)^2 \right) \right) \right\} \\
&+ \sum_{n=1}^M G_n \sigma_1 \left\{ E_n Q \left(\frac{\frac{\ln(\Gamma_1) - \mu_1}{\sigma_1} - E_n}{S_n} \right) + S_n^2 \left(\frac{1}{\sqrt{2\pi S_n^2}} \exp \left(-\frac{1}{2} \left(\frac{\frac{\ln(\Gamma_1) - \mu_1}{\sigma_1} - E_n}{S_n} \right)^2 \right) \right) \right\} \\
&+ \sum_{n=1}^M G_n \mu_1 Q \left(\frac{\frac{\ln(\Gamma_1) - \mu_1}{\sigma_1} - E_n}{S_n} \right) + \sum_{n=1}^M H_n \sigma_2 \left\{ F_n Q \left(\frac{\frac{\ln(\Gamma_2) - \mu_2}{\sigma_2} - F_n}{T_n} \right) \right. \\
&\left. + T_n^2 \left(\frac{1}{\sqrt{2\pi T_n^2}} \exp \left(-\frac{1}{2} \left(\frac{\frac{\ln(\Gamma_2) - \mu_2}{\sigma_2} - F_n}{T_n} \right)^2 \right) \right) \right\} + \sum_{n=1}^M H_n \mu_2 Q \left(\frac{\frac{\ln(\Gamma_2) - \mu_2}{\sigma_2} - F_n}{T_n} \right). \tag{29}
\end{aligned}$$

B. ISDF

The average channel capacity for the system with the ISDF strategy can be calculated by summing up the average channel capacities of the following events: i) the average channel capacity of the direct link when the SD link SNR meets the threshold requirement, ii) the average channel capacity of the relayed transmission when the SD link SNR fails to meet the threshold requirement and the SR link SNR satisfies the threshold requirement, and iii) if the SR link fails to achieve the SNR threshold, we assume that some rate can be achieved through the direct link even though its SNR is below Γ_0 . The last event ensures spectral efficiency of the ISDF system by not allowing the relay to participate if the SR link has poor SNR. Thus, the end-to-end average channel capacity can be expressed as

$$\begin{aligned} \mathcal{C}_{\text{ISDF}} &= \mathbb{E}[\mathcal{C}(\gamma_0|\gamma_0 > \Gamma_0)] + \frac{1}{2}\Pr[\gamma_0 < \Gamma_0]\mathbb{E}[\mathcal{C}(\gamma_m|\gamma_1 > \Gamma_1)] \\ &\quad + \Pr[\gamma_1 < \Gamma_1]\mathbb{E}[\mathcal{C}(\gamma_0|\gamma_0 < \Gamma_0)]. \end{aligned} \quad (22)$$

The PDF of $\{\gamma_m|\gamma_1 > \Gamma_1\}$ needs to be found out before evaluating the average capacity. Events $\{\gamma_m\}$ and $\{\gamma_1 > \Gamma_1\}$ are not independent, as $\gamma_m = \min\{\gamma_1, \gamma_2\}$. Hence, the PDF of $\{\gamma_m|\gamma_1 > \Gamma_1\}$ can be expressed as

$$\begin{aligned} &f_{\gamma_m|\gamma_1 > \Gamma_1}(x) \\ &= \begin{cases} Q\left(\frac{\ln \Gamma_1 - \mu_1}{\sigma_1}\right) \frac{1}{x\sqrt{2\pi\sigma_2^2}} \exp\left(-\frac{1}{2}\left(\frac{\ln x - \mu_2}{\sigma_2}\right)^2\right) & x \leq \Gamma_1; \\ Q\left(\frac{\ln x - \mu_1}{\sigma_1}\right) \frac{1}{x\sqrt{2\pi\sigma_2^2}} \exp\left(-\frac{1}{2}\left(\frac{\ln x - \mu_2}{\sigma_2}\right)^2\right) \\ + Q\left(\frac{\ln x - \mu_2}{\sigma_2}\right) \frac{1}{x\sqrt{2\pi\sigma_1^2}} \exp\left(-\frac{1}{2}\left(\frac{\ln x - \mu_1}{\sigma_1}\right)^2\right) & x > \Gamma_1. \end{cases} \end{aligned} \quad (23)$$

To evaluate (22) in closed-form is difficult as integrals over the PDF obtained above should be solve. Hence, either the Gaussian Q -function or the PDF itself needs to be approximated. Several approximations exist in the literature for the Gaussian Q -function, e.g., in [27], [28]. However, these approximations are mathematically intractable in this case. Instead, by utilizing an approximation provided in [29] which uses only a single Gaussian function, we develop an approximation method with multiple Gaussian functions using non-linear least-square curve fitting technique as

$$Q(x) \approx \sum_{n=1}^N \Phi_n \exp\left(-\left(\frac{x - \Psi_n}{\Omega_n}\right)^2\right), \quad (24)$$

where Φ_n , Ψ_n , and Ω_n are fitting constants. Compared to the approximation provided in [29], our approximation is more accurate as well as mathematically tractable. The number of summation terms, N , depends on the region of interest and accuracy of the fit. A suitable value of N and corresponding Φ_n , Ψ_n , and Ω_n are discussed later, in the results section. Using this approximation and the terms defined in (25), the end-to-end average channel capacity for the ISDF strategy can be evaluated as

$$\mathcal{C}_{\text{ISDF}} = \frac{\ln(\tau_1^{\Lambda_1} \tau_2^{\Lambda_2})}{\ln(2)} \left\{ Q\left(\frac{\ln(\Gamma_0) - \mu_0}{\sigma_0}\right) \right.$$

$$\begin{aligned}
& + \left(1 - Q \left(\frac{\ln(\Gamma_1) - \mu_1}{\sigma_1} \right) \right) \left(1 - Q \left(\frac{\ln(\Gamma_0) - \mu_0}{\sigma_0} \right) \right) \\
& + \frac{1}{2} \left(1 - Q \left(\frac{\ln(\Gamma_0) - \mu_0}{\sigma_0} \right) \right) \left(Q \left(\frac{\ln(\Gamma_1) - \mu_1}{\sigma_1} \right) \right) \Big\} \\
& + \frac{1}{\ln(2)} \left\{ I_4 + \left(1 - Q \left(\frac{\ln(\Gamma_1) - \mu_1}{\sigma_1} \right) \right) I_5 \right. \\
& \left. + \frac{1}{2} \left(1 - Q \left(\frac{\ln(\Gamma_0) - \mu_0}{\sigma_0} \right) \right) I_6 \right\}, \tag{26}
\end{aligned}$$

where I_4 , I_5 , and I_6 are given by (27), (28), and (29), respectively, shown at the bottom of the page.

IV. OUTAGE PROBABILITY

The outage probability is defined as the probability that the instantaneous channel capacity at the destination falls below a predefined rate. In other words, when the SNR threshold requirement corresponding to the rate is not fulfilled, outage occurs. In this section, we obtain the outage probabilities for the IDF and ISDF strategies in closed-form.

A. IDF

An outage event occurs if i) the SD link fails to achieve the required rate of R_{th} , and ii) in the relayed transmission, the minimum of the SR and the RD links SNRs fails to achieve twice the required rate (as the relay is half-duplex). Thus, the outage probability can be mathematically obtained by multiplying the probabilities of events i) and ii) as

$$\begin{aligned}
\mathcal{P}_{\text{IDF}}(R_{th}) & = \Pr[\gamma_0 < \Gamma_0] \times \Pr[\gamma_m < \Gamma_{th}] \\
& = \Pr[\gamma_0 < \Gamma_0] (1 - \Pr[\gamma_1 > \Gamma_{th}] \Pr[\gamma_2 > \Gamma_{th}]) \\
& = Q \left(\frac{\mu_0 - \ln(\Gamma_0)}{\sigma_0} \right) \left(1 - \left(Q \left(\frac{\ln(\Gamma_{th}) - \mu_1}{\sigma_1} \right) \right. \right. \\
& \left. \left. \times Q \left(\frac{\ln(\Gamma_{th}) - \mu_2}{\sigma_2} \right) \right) \right). \tag{30}
\end{aligned}$$

$$\mathcal{P}_{\text{ISDF}}(R_{th}) = \begin{cases} Q \left(\frac{\mu_0 - \ln \Gamma_0}{\sigma_0} \right) Q \left(\frac{\mu_1 - \ln \Gamma_1}{\sigma_1} \right) + Q \left(\frac{\mu_0 - \ln \Gamma_0}{\sigma_0} \right) Q \left(\frac{\ln \Gamma_1 - \mu_1}{\sigma_1} \right) Q \left(\frac{\mu_2 - \ln \Gamma_{th}}{\sigma_2} \right) & \text{for } \Gamma_1 \geq \Gamma_{th}; \\ Q \left(\frac{\mu_0 - \ln \Gamma_0}{\sigma_0} \right) Q \left(\frac{\mu_1 - \ln \Gamma_1}{\sigma_1} \right) + Q \left(\frac{\mu_0 - \ln \Gamma_0}{\sigma_0} \right) Q \left(\frac{\ln \Gamma_{th} - \mu_1}{\sigma_1} \right) Q \left(\frac{\mu_2 - \ln \Gamma_{th}}{\sigma_2} \right) & \\ + Q \left(\frac{\mu_0 - \ln \Gamma_0}{\sigma_0} \right) \left(Q \left(\frac{\ln \Gamma_1 - \mu_1}{\sigma_1} \right) - Q \left(\frac{\ln \Gamma_{th} - \mu_1}{\sigma_1} \right) \right) & \text{for } \Gamma_1 < \Gamma_{th} \end{cases} \tag{32}$$

B. ISDF

An outage event occurs if i) the SD link fails to achieve the required rate of R_{th} , and ii) either the relayed transmission is overruled, or if the relayed transmission happens, it fails to achieve the required rate. Thus,

$$\begin{aligned} \mathcal{P}_{\text{ISDF}}(R_{th}) &= \Pr[\gamma_0 < \Gamma_0] \\ &\times (\Pr[\gamma_1 < \Gamma_1] + \Pr[\gamma_m < \Gamma_{th} | \gamma_1 \geq \Gamma_1]). \end{aligned} \quad (31)$$

Based on the values of Γ_{th} and Γ_1 , the outage probability can be expressed in closed-form as in (32), placed at the bottom of this page.

It is interesting to observe that if Γ_1 is set to Γ_{th} , outage probabilities for the IDF and ISDF strategies in (30) and (32), respectively, become the same.

V. AVERAGE BIT ERROR RATE

In this section, we derive the average BER expressions for the relaying schemes assuming binary phase-shift keying (BPSK) signaling.

A. IDF

According to the IDF strategy under consideration, a bit error can occur either in the direct or in the relayed transmission to D . A bit error in the direct transmission can occur even if its SNR exceeds the required threshold. Now, a bit error in the relayed transmission can occur only if one of the links between the SR or the RD is in error when the SD link SNR does not meet the required threshold. Thus, the average BER for binary signaling can therefore be obtained by summing up the probabilities of all the above events as

$$BER_{\text{IDF}} = \mathbb{E}[P_e(\gamma_0 | \gamma_0 \geq \Gamma_0)] + \Pr[\gamma_0 < \Gamma_0]$$

$$\begin{aligned} BER_{\text{IDF}} &= \sum_{n=1}^M \sum_{j=1}^2 \frac{2 \Lambda_j \alpha_n}{\sigma_0 \sqrt{2} A_{n,1}} \exp\left(-\left(C_{n,j,1} - \left(\frac{B_{n,j,1}}{A_{n,1}}\right)^2\right)\right) \left[Q\left(\sqrt{2}\left(A_{n,1} \ln(\sqrt{\tau_j} \Gamma_0) - \frac{B_{n,j,1}}{A_{n,1}}\right)\right)\right] \\ &+ \left(1 - Q\left(\frac{\ln \Gamma_0 - \mu_0}{\sigma_0}\right)\right) \left\{ \left(1 - \sum_{n=1}^M \sum_{j=1}^2 \frac{2 \Lambda_j \alpha_n}{\sigma_1 \sqrt{2} A_{n,2}} \exp\left(-\left(C_{n,j,2} - \left(\frac{B_{n,j,2}}{A_{n,2}}\right)^2\right)\right)\right) \right. \\ &\times \left(\sum_{n=1}^M \sum_{j=1}^2 \frac{2 \Lambda_j \alpha_n}{\sigma_2 \sqrt{2} A_{n,3}} \exp\left(-\left(C_{n,j,3} - \left(\frac{B_{n,j,3}}{A_{n,3}}\right)^2\right)\right)\right) + \left(\sum_{n=1}^M \sum_{j=1}^2 \frac{2 \Lambda_j \alpha_n}{\sigma_1 \sqrt{2} A_{n,2}} \right. \\ &\left. \left. \times \exp\left(-\left(C_{n,j,2} - \left(\frac{B_{n,j,2}}{A_{n,2}}\right)^2\right)\right)\right) \left(1 - \sum_{n=1}^M \sum_{j=1}^2 \frac{2 \Lambda_j \alpha_n}{\sigma_2 \sqrt{2} A_{n,3}} \exp\left(-\left(C_{n,j,3} - \left(\frac{B_{n,j,3}}{A_{n,3}}\right)^2\right)\right)\right) \right\}. \end{aligned} \quad (39)$$

$$\begin{aligned}
& \times ((1 - \mathbb{E}[P_e(\gamma_1)]) \mathbb{E}[P_e(\gamma_2)] \\
& + \mathbb{E}[P_e(\gamma_1)] (1 - \mathbb{E}[P_e(\gamma_2)])) .
\end{aligned} \tag{33}$$

In the above expression, we have discarded the event of two consecutive error detection in relayed transmission as this would result in a correct decision at the destination for BPSK.

For equiprobable BPSK signaling scheme, $P_e(v)$ is given by [12]

$$P_e(x) = \sum_{j=1}^2 \Lambda_j Q(\sqrt{\tau_j x}) . \tag{34}$$

Thus, to get a closed-form solution for (33), we need the solution of the following type of integral

$$\begin{aligned}
& \mathbb{E}[P_e(x|x_1 < X \leq x_2)] \\
& = \sum_{j=1}^2 \int_{x_1}^{x_2} \Lambda_j Q(\sqrt{\tau_j x}) \\
& \times \frac{1}{x\sqrt{2\pi\sigma_i^2}} \exp\left(-\frac{1}{2} \left(\frac{\ln(x) - \mu_i}{\sigma_i}\right)^2\right) dx \\
& = \sum_{j=1}^2 \int_{\ln(\sqrt{\tau_j x_1})}^{\ln(\sqrt{\tau_j x_2})} \Lambda_j Q(\exp(t)) \\
& \times \frac{2}{\sqrt{2\pi\sigma_i^2}} \exp\left(-\frac{1}{2} \left(\frac{2t - \ln(\tau_j) - \mu_i}{\sigma_i}\right)^2\right) dt .
\end{aligned} \tag{35}$$

It is difficult to evaluate the above integral in closed-form, as it contains a function of the form $Q(\exp(x))$. Therefore,

$$\begin{aligned}
BER_{\text{ISDF}} & = \sum_{n=1}^M \sum_{j=1}^2 \frac{2\Lambda_j \alpha_n}{\sigma_0 \sqrt{2} A_{n,1}} \exp\left(-\left(C_{n,j,1} - \left(\frac{B_{n,j,1}}{A_{n,1}}\right)^2\right)\right) \left[Q\left(\sqrt{2} \left(A_{n,1} \ln(\sqrt{\tau_j} \Gamma_0) - \frac{B_{n,j,1}}{A_{n,1}}\right)\right)\right] \\
& + \left(1 - Q\left(\frac{\ln \Gamma_1 - \mu_1}{\sigma_1}\right)\right) \sum_{n=1}^M \sum_{j=1}^2 \frac{2\Lambda_j \alpha_n}{\sigma_0 \sqrt{2} A_{n,1}} \exp\left(-\left(C_{n,j,1} - \left(\frac{B_{n,j,1}}{A_{n,1}}\right)^2\right)\right) \\
& \times \left[1 - Q\left(\sqrt{2} \left(A_{n,1} \ln(\sqrt{\tau_j} \Gamma_0) - \frac{B_{n,j,1}}{A_{n,1}}\right)\right)\right] + \left(1 - Q\left(\frac{\ln \Gamma_0 - \mu_0}{\sigma_0}\right)\right) \\
& \times \left\{ \left(1 - \sum_{n=1}^M \sum_{j=1}^2 \frac{2\Lambda_j \alpha_n}{\sigma_1 \sqrt{2} A_{n,2}} \exp\left(-\left(C_{n,j,2} - \left(\frac{B_{n,j,2}}{A_{n,2}}\right)^2\right)\right)\right) \left(\sum_{n=1}^M \sum_{j=1}^2 \frac{2\Lambda_j \alpha_n}{\sigma_2 \sqrt{2} A_{n,3}}\right) \right. \\
& \times \exp\left(-\left(C_{n,j,3} - \left(\frac{B_{n,j,3}}{A_{n,3}}\right)^2\right)\right) \left(Q\left(\frac{\ln \Gamma_1 - \mu_1}{\sigma_1}\right)\right) \left. + \left(\sum_{n=1}^M \sum_{j=1}^2 \frac{2\Lambda_j \alpha_n}{\sigma_1 \sqrt{2} A_{n,2}}\right) \right. \\
& \times \exp\left(-\left(C_{n,j,2} - \left(\frac{B_{n,j,2}}{A_{n,2}}\right)^2\right)\right) \left(1 - \sum_{n=1}^M \sum_{j=1}^2 \frac{2\Lambda_j \alpha_n}{\sigma_2 \sqrt{2} A_{n,3}} \exp\left(-\left(C_{n,j,3} - \left(\frac{B_{n,j,3}}{A_{n,3}}\right)^2\right)\right)\right) \left(Q\left(\frac{\ln \Gamma_1 - \mu_1}{\sigma_1}\right)\right) \right\}
\end{aligned} \tag{41}$$

using the same curve fitting technique proposed in the Section III-B, the approximation of the function $Q(\exp(x))$ is given by

$$Q(\exp(x)) \approx \sum_{n=1}^M \alpha_n \exp\left(-\left(\frac{x - \beta_n}{\delta_n}\right)^2\right), \quad (36)$$

where α_n, β_n , and δ_n are fitting constants. The number of summation terms, M , depends on the region of interest and accuracy of the fit. Using this approximation, the integral in (35) can be evaluated in closed-form as

$$\begin{aligned} & \mathbb{E}[P_e(x|x_1 < X \leq x_2)] \\ & \approx \sum_{n=1}^M \sum_{j=1}^2 \frac{2 \Lambda_j \alpha_n}{\sigma_i \sqrt{2} A_{n,i}} \exp\left(-\left(C_{n,j,i} - \left(\frac{B_{n,j,i}}{A_{n,i}}\right)^2\right)\right) \\ & \times \left\{ Q\left(\sqrt{2} \left(A_{n,i} \ln(\sqrt{\tau_j} x_1) - \frac{B_{n,j,i}}{A_{n,i}}\right)\right) \right. \\ & \left. - Q\left(\sqrt{2} \left(A_{n,i} \ln(\sqrt{\tau_j} x_2) - \frac{B_{n,j,i}}{A_{n,i}}\right)\right) \right\}, \quad (37) \end{aligned}$$

where

$$\begin{aligned} A_{n,i} &= \sqrt{\frac{1}{\delta_n^2} + \frac{2}{\sigma_i^2}}, \quad B_{n,j,i} = \frac{\beta_n}{\delta_n^2} + \frac{\ln(\tau_j) + \mu_i}{\sigma_i^2}, \\ C_{n,j,i} &= \frac{\beta_n^2}{\delta_n^2} + \frac{(\ln(\tau_j) + \mu_i)^2}{2\sigma_i^2}. \quad (38) \end{aligned}$$

Finally, using (12) and (37), the average BER in (33) can be expressed in approximate closed-form as in (39) at the bottom of the next page.

B. ISDF

The average BER for the system with ISDF strategy can be calculated by summing up the average BER of the following events: i) the average BER of the direct link when the SD link SNR meets the threshold requirement, ii) the average BER of the relayed transmission when the SD link SNR fails to fulfill the threshold requirement and the SR link SNR achieves the threshold requirement, and iii) if the SR link fails to achieve the SNR threshold, we assume that decision can be taken based on the symbol received through the direct link even though its SNR is below Γ_0 . Thus, the average BER for binary signaling can be obtained by summing up the probabilities of all the above events as

$$\begin{aligned} & BER_{\text{ISDF}} \\ &= \mathbb{E}[P_e(\gamma_0 | \gamma_0 \geq \Gamma_0)] \\ &+ \Pr[\gamma_0 < \Gamma_0] \left((1 - \mathbb{E}[P_e(\gamma_1 | \gamma_1 \geq \Gamma_1)]) \mathbb{E}[P_e(\gamma_2 | \gamma_1 \geq \Gamma_1)] \right. \\ &+ \mathbb{E}[P_e(\gamma_1 | \gamma_1 \geq \Gamma_1)] (1 - \mathbb{E}[P_e(\gamma_2 | \gamma_1 \geq \Gamma_1)]) \left. \right) \\ &+ \Pr[\gamma_1 < \Gamma_1] \mathbb{E}[P_e(\gamma_0 | \gamma_0 < \Gamma_0)]. \quad (40) \end{aligned}$$

TABLE I: Parameters for (24) and (36) from curve fitting for $M = N = 7$.

n	α_n	β_n	δ_n	Φ_n	Ψ_n	Ω_n
1	0.4665	-5.37	2.174	0.9302	-5.48	2.833
2	-0.0007029	-3.674	0.1178	0.0001404	-1.157	0.01036
3	0.0165	-3.141	0.0004957	0.0007985	-1.381	0.021
4	0.2831	-2.998	1.458	-0.001064	-0.9854	0.158
5	0.2113	-1.764	1.06	0.00196	-1.699	0.173
6	0.1742	-0.8425	0.837	0.4171	-0.7018	1.535
7	0.07986	-0.1109	0.6399	0.5843	-2.347	1.96

Using (12) and (37), the average BER in (40) can be expressed in approximate closed-form as in (41) at the bottom of the page.

VI. RELAY USAGE

The more the relay is used for data transmission, the poorer the spectral efficiency, and the more the additional complexity and delay required in data processing. However, the more the relay is used, the better the outage performance. Hence, in this section, *the fraction of times the relay is in use* is calculated for both IDF and ISDF strategies.

In the IDF, the relay is used only if the SD link SNR fails to attain the threshold requirement. Thus, the fraction of times the relay is in use can be obtained simply by finding the probability that the SD link SNR fails to attain the threshold requirement. In the ISDF, the relay is used if the SD link SNR fails to attain the threshold requirement while the SR link SNR attains it. Hence, the fraction of times the relay is in use for IDF and ISDF can be expressed as

$$N_{\text{IDF}} = \Pr[\gamma_0 < \Gamma_0] = 1 - Q\left(\frac{\ln(\Gamma_0) - \mu_0}{\sigma_0}\right), \quad (42)$$

$$\begin{aligned} N_{\text{ISDF}} &= \Pr[\gamma_0 < \Gamma_0] \Pr[\gamma_1 > \Gamma_1] \\ &= \left(1 - Q\left(\frac{\ln(\Gamma_0) - \mu_0}{\sigma_0}\right)\right) Q\left(\frac{\ln(\Gamma_1) - \mu_1}{\sigma_1}\right), \end{aligned} \quad (43)$$

respectively.

VII. OPTIMUM POWER ALLOCATION

Instead of allocating equal power to S and R , the power can be allocated judiciously to improve the system performance. In this section, we investigate the power allocation problem to minimize the outage probability. Towards this goal, we first check whether or not the outage probability is a convex function of the power allocation factor, p_f . Then, we find the global optimum power allocation factor [35]. One can observe from Section IV that the outage probability is the same for both IDF and ISDF when $\Gamma_1 = \Gamma_{th}$. Hence, power allocation is solved only for this case.

The outage probability in (30) can be expressed as a function of the power allocation factor, p_f , as

$$\begin{aligned}
\mathcal{P}_{IDF}(p_f) &= Q(v_0 \ln(p_f) - u_0) [Q(v_1 \ln(p_f) - u_1) \\
&\quad + Q(v_2 \ln(1 - p_f) - u_2)] - Q(v_0 \ln(p_f) - u_0) \\
&\quad \times Q(v_1 \ln(p_f) - u_1) Q(v_2 \ln(1 - p_f) - u_2), \tag{44}
\end{aligned}$$

where

$$v_i = \frac{1}{\sigma_i}, u_i = \frac{\ln(\Gamma_i) - 2\Xi_i - \ln(P_T/(N_0 P_L d_i))}{\sigma_i}. \tag{45}$$

As the Q -function values are always less than unity, the product of three Q -functions will be very small when compared to the other terms in (44). Hence, we get an approximation by neglecting this product, as

$$\begin{aligned}
\mathcal{P}_{IDF}(p_f) &= Q(v_0 \ln(p_f) - u_0) [Q(v_1 \ln(p_f) - u_1) \\
&\quad + Q(v_2 \ln(1 - p_f) - u_2)]. \tag{46}
\end{aligned}$$

The approximation is more accurate when the argument of the Q -function is positive and large at higher P_T . This approximation will help up to show the convexity of the power allocation problem easily, as opposed to the actual problem.

The first and second-order derivative of (46), with respect to p_f , are obtained as

$$\begin{aligned}
\mathcal{P}'_{IDF}(p_f) &= Q'(v_0 \ln(p_f) - u_0) [Q(v_1 \ln(p_f) - u_1) \\
&\quad + Q(v_2 \ln(1 - p_f) - u_2)] \\
&\quad + Q(v_0 \ln(p_f) - u_0) [Q'(v_1 \ln(p_f) - u_1) \\
&\quad + Q'(v_2 \ln(1 - p_f) - u_2)], \tag{47}
\end{aligned}$$

$$\begin{aligned}
\mathcal{P}''_{IDF}(p_f) &= Q''(v_0 \ln(p_f) - u_0) [Q(v_1 \ln(p_f) - u_1) \\
&\quad + Q(v_2 \ln(1 - p_f) - u_2)] \\
&\quad + 2Q'(v_0 \ln(p_f) - u_0) [Q'(v_1 \ln(p_f) - u_1) \\
&\quad + Q'(v_2 \ln(1 - p_f) - u_2)] \\
&\quad + 2Q(v_0 \ln(p_f) - u_0) [Q''(v_1 \ln(p_f) - u_1) \\
&\quad + Q''(v_2 \ln(1 - p_f) - u_2)], \tag{48}
\end{aligned}$$

where $Q'(\cdot)$ and $Q''(\cdot)$ denote the first and second-order derivative of the Q -function [34]. It is still difficult to confirm straightway that the approximate $\mathcal{P}''_{IDF}(p_f)$ is positive $\forall p_f$. Instead, we can show from (48) that when P_T is sufficiently high, $\mathcal{P}''_{IDF}(p_f)$ is positive. We can see from (45) that the arguments of Q -functions are positive, i.e., $(v_i \ln(p_f) - u_i) > 0$ and $(v_i \ln(1 - p_f) - u_i) > 0$. Thus, (48) can be easily shown to always be positive if P_T is

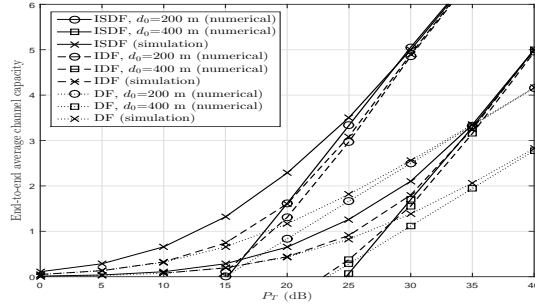


Fig. 3: End-to-end average channel capacity versus total transmit power with $\xi_i = 3$ dB, $P_L = 50$ dB/km, $p_f = 0.5$, $d_f = 0.1$, $\Lambda = 0.1$, $\eta = 10$, $R_{th} = 4$ bits/sec/Hz, and $\Gamma_1 = \Gamma_{th}$ for different d_0 .

sufficiently high so that the received SNR is greater than some quantity, i.e.,

$$P_T / (N_0 P_L d_2) > \exp(\max\{\theta_i, \phi_i\}),$$

where $\theta_i = \ln(\Gamma_i) - 2\Xi_i - v_i \ln(p_f)$ and $\phi_i = \ln(\Gamma_i) - 2\Xi_i - v_i \ln(1 - p_f)$.

At this point we have shown analytically that at sufficiently high SNR, the approximated $\mathcal{P}_{IDF}(p_f)$ is a convex function of p_f . Therefore, a global minimum for $\mathcal{P}_{IDF}(p_f)$ exists. By equating $\mathcal{P}'_{IDF}(p_f)$ to zero, p_f can be evaluated. It is, however, difficult to evaluate p_f in closed-form due to the complexity of the equation involved. Hence, we compute it numerically.

VIII. RESULTS AND DISCUSSIONS

Numerical and simulation results are presented in this section to validate the analysis. The distance between S and D is assumed to be between 200 and 400 meters. This range of distances best suits small PLC system environment, such as home automation and load control applications. Depending on the power distribution network (number of paths in multipath model), in general, ξ_i lies in between 2 dB to 5 dB [5]. High value of ξ_i indicates high fluctuation in the received signal power [4], [5]. Here, ξ_i is represented in dB, for all i , where the conversion from natural scale to dB scale is given by $\xi_i(\text{dB}) = 10\xi_i / \ln 10$. It has been shown that the path-loss in PLC ranges from 40 to 80 dB/km [32]; hence, $P_L = 50$ dB/km is chosen for the analysis. Unless otherwise specified, the value of the impulsive noise parameters are $\Lambda = 0.1$ and $\eta = 10$. For the approximation presented in (24), $N = 7$ is found to be sufficient with root mean squared error (RMSE) of 7.264×10^{-4} and sum of squares due to error (SSE) of 5.171×10^{-4} . Similarly, for (36), $M = 7$ is sufficient with RMSE of 6.931×10^{-4} and SSE of 4.708×10^{-4} for the curve fitting. The fitting constants corresponding to (24) and (36) are given in Table I. In this section, results in Figs. 3-8 are obtained using MATLAB, by averaging over 1 million channel realizations.

Fig. 3 compares the end-to-end average channel capacity of the proposed strategies with the traditional DF strategy. The numerical results for IDF and ISDF are obtained using the approximate closed-form expressions derived in (21) and (26), respectively. For traditional DF, it is obtained from [12]. Numerical results are in agreement with

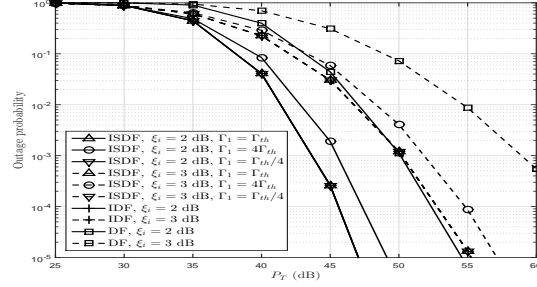


Fig. 4: Outage probability versus total transmit power with $d_0 = 400$ m, $P_L = 50$ dB/km, $\Lambda = 0.1$, $\eta = 10$, $R_{th} = 4$ bits/sec/Hz, $p_f = 0.5$, and $d_f = 0.5$ for various ξ_i and Γ_1 .

simulation results at high SNR, thus validating our high SNR approximate analysis. In general, Fig. 3 shows that for a given P_T , the average channel capacity decreases with the increase in d_0 due to the path loss.

It can be seen that, at relatively low P_T , the ISDF has the highest average channel capacity and DF has the lowest, at a given d_0 . Though both IDF and ISDF are incremental relaying techniques, as there is an extra check on the SNR at R for ISDF, its capacity is greater than that of IDF. On the other hand, average channel capacity of the traditional DF relaying is the lowest, as it is not an incremental relaying technique. Furthermore, average capacity performances become the same for all strategies at relatively high P_T as they all follow direct transmission. Moreover, by checking the average capacity at $d_0 = 200$ m, we observe that ISDF achieves $R_{th} = 4$ bits/sec/Hz at a lower P_T than IDF. However, at $d_0 = 400$ m, both require the same P_T . Thus, it can be concluded that ISDF outperforms IDF at comparatively low P_T and d_0 .

Fig. 4 shows the outage probability versus P_T for the proposed strategies by changing Γ_1 for a given ξ_i . The general observations illustrate that to achieve a desired outage performance, the total transmit power requirement increases with the increase in ξ_i . For example, for $\Gamma_1 = \Gamma_{th}$, to achieve an outage probability of 10^{-3} , the ISDF requires approximately 7 dB more SNR at $\xi_i = 3$ as compared to $\xi_i = 2$. This is reasonable because as the channel quality degrades, the transmit power requirement increases to achieve the same performance. It is also seen that when Γ_1 is less than Γ_{th} , the outage performance remains the same with the increase in Γ_1 . However, the outage performance degrades with increasing Γ_1 beyond Γ_{th} . As Γ_1 increases while remaining below Γ_{th} , the relay usage decreases. However, it does not change the outage performance because all relayed transmissions with $\Gamma_1 \leq \gamma_1 < \Gamma_{th}$ will be in outage as per the definition in Section IV. On the other hand, if Γ_1 is beyond Γ_{th} , the relay will force the system to go into outage by blocking the transmissions with $\Gamma_{th} < \gamma_1 \leq \Gamma_1$. When $\Gamma_1 = \Gamma_{th}$, both the IDF and the ISDF have identical outage performance. Thus, it can be concluded that ISDF behaves the same as IDF when $\Gamma_1 \leq \Gamma_{th}$.

Fig. 5 shows the average BER versus P_T for the proposed strategies and the traditional DF strategy for different R_{th} . The numerical results for the IDF and ISDF strategies are obtained using the approximate closed-form expressions derived in (39) and (41), respectively, whereas results for the traditional dual-hop DF scheme are obtained from [12]. Numerical results are in agreement with simulation results, thus validating our analysis. In

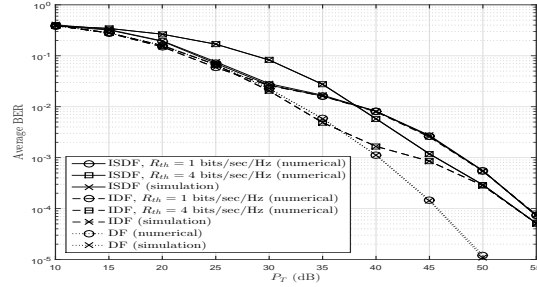
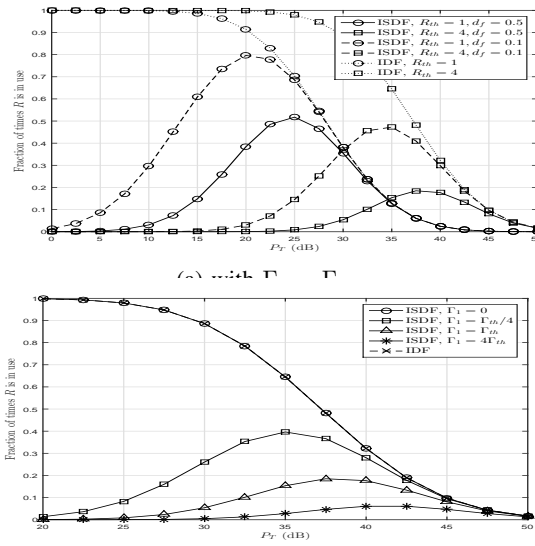


Fig. 5: Average BER versus total transmit power with $\xi_i = 3$ dB, $d_0 = 400$ m, $P_L = 50$ dB/km, $p_f = 0.5$, $d_f = 0.5$, $\Lambda = 0.1$, $\eta = 10$, and $\Gamma_1 = \Gamma_{th}$ for different R_{th} .



(b) with $d_f = 0.5$ and $R_{th} = 4$ bits/sec/Hz

Fig. 6: Fraction of times R is in use versus P_T with $\xi_i = 3$ dB, $d_0 = 400$ m, $P_L = 50$ dB/km, $p_f = 0.5$, $\Lambda = 0.1$, and $\eta = 10$ for (a) different R_{th} and d_f values and (b) different Γ_1 values.

general, Fig. 5 shows that the average BER improves with the increase in P_T . Furthermore, for the proposed strategies, it can be seen that when P_T is low, the average BER degrades with the increase in R_{th} ; however, when P_T is high, it improves with the increase in R_{th} . Moreover, at very high P_T , the BER curves merge for different R_{th} . This is because the system tends to follow the direct transmission at such high P_T values. This is an interesting observation as with the increase in R_{th} , intuitively, the average BER should degrade at all SNRs. When R_{th} increases, the average BER decreases at a lower P_T as neither the SD nor the SR can overcome the increased SNR threshold at D and R , respectively. If P_T is increased further, R can eventually overcome the required SNR threshold due to comparatively low path loss and increased received power at it, hence, this observation. Furthermore, it can be observed that the traditional DF is superior over the proposed strategies. The traditional DF, however, has very low spectral efficiency (to be discussed later in detail).

In Figs. 6a and 6b, the fraction of times R is in use for transmission versus P_T is plotted for the proposed strategies using (42) and (43), respectively, by varying R_{th} , d_f , and Γ_1 . Observations reveal that with the increase in P_T , the curves for IDF are approaching zero from unity. On the other hand, the curves for ISDF are bell-shaped and never reach unity. Initially, R is used every time when the SD link fails to achieve R_{th} at low SNR in IDF. Later, with the increase in P_T , the relayed transmission ceases, and hence the observation. However, due to threshold-selection, the relay usage never achieves unity in ISDF. As P_T increases, the relay usage initially increases due to improved SR link quality, and then decreases due to better direct link quality, and hence, the bell-shaped curves for ISDF.

Next, Fig. 6a illustrates for the ISDF strategy that as d_f increases at a given R_{th} , the corresponding curves shift towards the right and its maximum also reduces. As the length of the SR link increases, the received SNR at R decreases, which in turn reduces N_{ISDF} . On the other hand, in the IDF strategy, R is used every time irrespective of its placement as there is no threshold-selection.

Furthermore, as N_{ISDF} is always less than or equal to N_{IDF} , the average channel capacity of the ISDF is always more than or equal to that of IDF in Fig. 3. Thus, it can be concluded that ISDF is spectrally more efficient than both the IDF and the traditional DF relaying.

Moreover, we can observe that in the case of ISDF strategy at a given d_f and beyond a certain P_T , N_{ISDF} for $R_{th} = 4$ becomes more than that for $R_{th} = 1$ due to the bell-shape. This justifies the crossovers of the average BER plots for the same d_f in Fig. 5. Thus, although the spectral efficiency decreases at higher P_T when R_{th} increases, interestingly, the average BER improves. On the contrary, in case of the IDF strategy, N_{IDF} for $R_{th} = 1$ is always less than that for $R_{th} = 4$. This justifies the nature of the BER curves in Fig. 5 for IDF.

Fig. 6b shows that as Γ_1 increases, the average relay usage decreases. Moreover, by comparing the observations in Figs. 4 and 6b, it can be concluded that increasing the value of Γ_1 while keeping it below Γ_{th} improves the spectral efficiency without compromising the outage performance. However, increasing its value beyond Γ_{th} degrades the outage performance. Thus, it can be concluded that using ISDF with $\Gamma_1 = \Gamma_{th}$ maximizes the spectral efficiency without compromising the outage performance.

In Fig. 7, the outage probability and its first-order derivative ($\mathcal{P}'_{IDF}(p_f)$) and second-order derivative ($\mathcal{P}''_{IDF}(p_f)$) are shown as a function of power allocation factors for different preassigned distances d_1 and d_2 . Clearly, the figure shows that the second-order derivative of the outage probability is always positive, confirming the convexity of the outage probability. The points at which the first-order derivative becomes zero, which is shown by circles, is the point at which minimum is achieved in $\mathcal{P}_{IDF}(p_f)$. Interestingly, we can observe that the minimum point on $\mathcal{P}_{IDF}(p_f)$ shifts towards right as d_f increases from 0.1 to 0.9. This means that as the distance between S and R increases, more power should be allocated to S . This is reasonable since as d_1 increases, the path loss degrades the SR link, and hence, more power should be assigned to S to compensate for the loss and minimize the outage probability.

Fig. 8a depicts $\mathcal{P}_{IDF}(p_f)$ with respect to p_f for different SD channel parameter at a given SR and RD channel quality, whereas Fig. 8b displays the same for different SR and RD channel parameters at a given SD channel quality. The purpose of this figure is two fold: first, it shows how the direct link from S to D affects the power

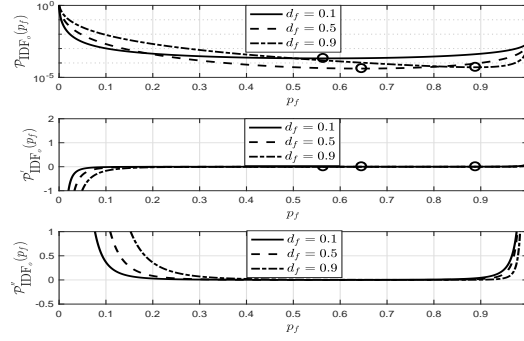


Fig. 7: Outage probability, first-order and second-order derivative of the outage probability versus p_f for different d_1 with $P_T = 50$ dB, $\xi_i = 4$ dB $\forall i$, $d_0 = 200$ m, $P_L = 80$ dB/km, $\Lambda = 0.1$, $\eta = 10$, $R_{th} = 2$, and $\Gamma_1 = \Gamma_{th}$.

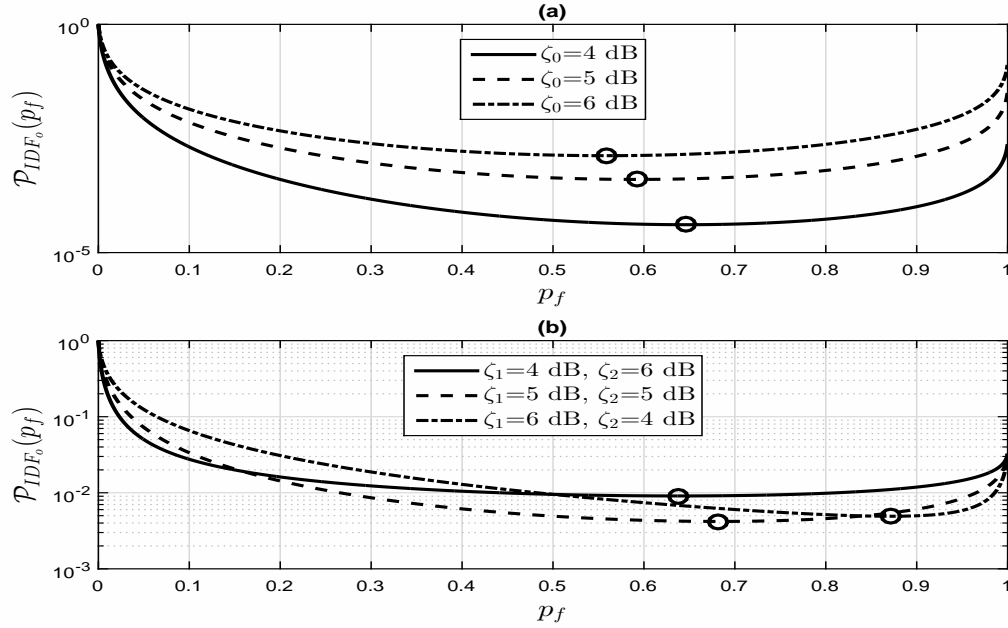


Fig. 8: Outage probability versus p_f when imbalance in channel parameters with $P_T = 50$ dB, $d_0 = 200$ m, $P_L = 80$ dB/km, $\Lambda = 0.1$, $\eta = 10$, $R_{th} = 2$, $d_f = 0.5$, and $\Gamma_1 = \Gamma_{th}$ when (a) $\xi_1 = \xi_2 = 4$ dB and (b) $\xi_0 = 5$ dB.

allocation when the relayed channel is balanced with equal SR and RD channel parameters, and secondly, it shows how the power allocation is affected when the relayed channel is imbalanced with unequal SR and RD channel quality at a given direct link channel quality. From Fig. 8a, we can observe that as the direct link deteriorates due to the increase in channel parameters, the minimum point shifts towards right. This means that to minimize the outage, more and more power should be allocated to S as the direct link quality worsens.

Fig. 8b illustrates that if the SR channel quality is inferior compared to the RD channel quality, the minimum point on outage probability is shifted towards right. This means that more power should be assigned to S if the

SR channel quality is worse compared to the RD channel quality. Thus, from the two cases, Figs. 8a and 8b, it can be concluded that more power should be allocated to S to first secure the SR transmission when compared to RD . This is because in an incremental relaying scheme with DF relays, if the first link can not maintain a proper rate of transmission, an outage is bound to happen even if the second link is better. By increasing the power at S , the direct transmission has better probability of success, and hence, the spectral efficiency increases.

Another point to be noticed from Fig. 8 is that even if SR , RD , and SD channel parameters are the same, the power allocation should not be equal, i.e., the optimum p_f is not 0.5, rather higher than 0.5. This is because for the same channel parameters even if SR and RD distances are the same, the path loss for SD is always more than the other two path losses and must be compensated by providing more power to S . Thus, the power allocation must be designed as per the inter-node distances along with the channel parameters.

IX. CONCLUSION

In this work, incremental relaying strategies have been introduced for the PLC system to improve spectral efficiency. Log-normal channel gain, Bernoulli-Gaussian impulsive noise, and distance-dependent attenuation are considered. Closed-form expressions for the outage probability and fraction of times the relay is in use, along with approximate closed-form expressions for the end-to-end average channel capacity and the bit error rate for BPSK signaling are derived. Observations show that at lower transmit power, the performance degrades as the required rate increases, while the converse happens at higher transmit power. The ISDF can achieve optimal spectral efficiency by choosing an appropriate threshold without compromising the performance. Power allocation studies reveal that power should be allocated according to the channel parameters and inter-node distances and not equally. We conclude that even if the relaying channels are identical, more than 50% of the total power should be allocated to the source to minimize the outage probability.

REFERENCES

- [1] H. C. Ferreira, L. Lampe, J. Newbury, and T. G. Swart, *Power Line Communications: Theory and Applications for Narrowband and Broadband Communications over Power Lines*, Singapore: Wiley, 2010.
- [2] L. de M. B. A. Dib, V. Fernandes, M. de L. Filomeno, and M. V. Ribeiro, "Hybrid PLC/wireless communication for smart grids and internet of things applications," *IEEE Internet Things J.*, vol. 5, no. 2, pp. 655–667, Apr. 2018.
- [3] Y. Qian et al., "Design of hybrid wireless and power line sensor networks with dual-interface relay in IoT," *IEEE Internet Things J.*, through early access.
- [4] I. C. Papaleonidopoulos, C. N. Capsalis, C. G. Karagiannopoulos, and N. J. Theodorou, "Statistical analysis and simulation of indoor single-phase low voltage power-line communication channels on the basis of multipath propagation," *IEEE Trans. Consum. Electron.*, vol. 49, no. 1, pp. 89–99, Feb. 2003.
- [5] S. Guzelgoz, H. B. Celebi, and H. Arslan, "Statistical characterization of the paths in multipath PLC channels," *IEEE Trans. Power Deliv.*, vol. 26, no. 1, pp. 181–187, Jan. 2011.
- [6] S. Galli, "A novel approach to the statistical modeling of wireline channels," *IEEE Trans. Commun.*, vol. 59, no. 5, pp. 1332–1345, May 2011.
- [7] A. Dubey, D. Sharma, R. K. Mallik, and S. Mishra, "Modeling and performance analysis of a PLC system in presence of impulsive noise," in *Proc. IEEE Power & Energy Society General Meeting*, Denver, Colorado, USA, 2015, pp. 1–5.

- [8] L. Lampe and A. J. Han Vinck, "On cooperative coding for narrow band PLC networks," *International Journal of Electronics and Communications*, vol. 65, no. 8, pp. 681–687, Aug. 2011.
- [9] L. Lampe, R. Schober, and S. Yiu, "Distributed space-time coding for multihop transmission in power line communication networks," *IEEE J. Sel. Areas Commun.*, vol. 24, no. 7, pp. 1389–1400, Jul. 2006.
- [10] X. Cheng, R. Cao, and L. Yang, "Relay-aided amplify-and-forward powerline communications," *IEEE Trans. Smart Grid*, vol. 4, no. 1, pp. 265–272, Mar. 2013.
- [11] S.-G. Yoon, S. Jang, Y.-H. Kim, and S. Bahk, "Opportunistic routing for smart grid with power line communication access networks," *IEEE Trans. Smart Grid*, vol. 5, no. 1, pp. 303–3011, Jan. 2014.
- [12] A. Dubey, R. K. Mallik, and R. Schober, "Performance analysis of a multi-hop power line communication system over log-normal fading in presence of impulsive noise," *IET Commun.*, vol. 9, no. 1, pp. 1–9, Jan. 2015.
- [13] A. Dubey and R. K. Mallik, "PLC system performance with AF relaying," *IEEE Trans. Commun.*, vol. 63, no. 6, pp. 2337–2345, Jun. 2015.
- [14] B. Nikfar and A. J. Han Vinck, "Relay selection in cooperative power line communication: A multi-armed bandit approach," *Journal of Communications and Networks*, vol. 19, no. 1, pp. 1–9, Feb. 2017.
- [15] K. M. Rabie, B. Adebisi, A. M. Tonello and G. Naurzybayev, "More robust decode-and-forward relaying over impulsive noise power line channels," in *Proc. 2017 IEEE International Symposium on Power Line Communications and its Applications (ISPLC)*, Madrid, 2017, pp. 1–5.
- [16] K. M. Rabie, B. Adebisi and H. Gacanin, "Outage probability and energy efficiency of DF relaying power line communication networks: Cooperative and non-cooperative," in *Proc. 2017 IEEE International Conference on Communications (ICC)*, Paris, 2017, pp. 1–6.
- [17] V. Fernandes, H. V. Poor, and M. V. Ribeiro, "Analyses of the incomplete low-lit-rate hybrid PLC-wireless single-relay channel," *IEEE Internet Things J.*, vol. 5, no. 2, pp. 917–929, Apr. 2018.
- [18] K. J. R. Liu, A. K. Sadek, W. Su, and A. Kwasinski, *Cooperative Communications and Networking*, New York: Cambridge University Press, 2008.
- [19] J. N. Laneman, D. N. C. Tse, and G. W. Wornell, "Cooperative diversity in wireless networks: Efficient protocols and outage behavior", *IEEE Trans. Inf. Theory*, vol. 50, no. 12, pp. 3062-3080, Dec. 2004.
- [20] K. S. Hwang, Y. C. Ko, and M. S. Alouini, "Performance analysis of incremental relaying with relay selection and adaptive modulation over non-identically distributed cooperative paths," *IEEE Trans. Wireless Commun.*, vol. 8, no. 4, pp. 1953-1961, Apr. 2009.
- [21] S. Ikki and M. H. Ahmed, "Performance analysis of incremental relaying cooperative diversity networks over Rayleigh fading channels," *IET Commun.*, vol. 5, no. 3, pp. 337-349, Feb. 2011.
- [22] Z. Bai, J. Jia, C.-X. Wang, and D. Yuan, "Performance analysis of SNR-based incremental hybrid decode-amplify-forward cooperative relaying protocol," *IEEE Trans. Commun.*, vol. 63, no. 6, pp. 2094-2106, Jun. 2015.
- [23] P. Holgate, "The lognormal characteristic function", *Communications in Statistical-Theory and Methods*, vol. 18, no. 12, pp. 4539–4548, Jun. 1989.
- [24] A. Dubey, C. Kundu, T. M. N. Ngatched, O. A. Dobre, and R. K. Mallik, "Incremental selective decode-and-forward relaying for power line communication," in *Proc. IEEE 86th Vehicular Technology Conference (VTC-Fall) 2017*, Toronto, ON, Canada, 2017, pp. 1-6.
- [25] Y. H. Ma, P. L. So, and E. Gunawan, "Performance analysis of OFDM systems for broadband power line communications under impulsive noise and multipath effects," *IEEE Trans. Power Deliv.*, vol. 20, no. 2, pp. 674–682, Apr. 2005.
- [26] M. Gotz, M. Rapp, and K. Dostert, "Power line channel characteristics and their effect on communication system design," *IEEE Commun. Mag.*, vol. 42, no. 4, pp. 78–86, Apr. 2004.
- [27] G. K. Karagiannidis and A. S. Lioumpas, "An improved approximation for the Gaussian Q-function," *IEEE Commun. Lett.*, vol. 11, no. 8, pp. 644–646, Aug. 2007.
- [28] Y. Isukapalli and B. D. Rao, "An analytically tractable approximation for the Gaussian Q-function," *IEEE Commun. Lett.*, vol. 12, no. 9, pp. 669–671, Sep. 2008.
- [29] M. Lopez-Benitez and F. Casadevall, "Versatile, accurate, and analytically tractable approximation for the Gaussian Q-function," *IEEE Trans. Commun.*, vol. 59 no. 4, pp. 917–922, Apr. 2011.
- [30] M. K Simon, *Probability Distributions Involving Gaussian Random Variables: A Handbook for Engineers and Scientists*, Kluwer, 2002.
- [31] K. C. Wiklundh, P. F. Stenumgaard, and H. M. Tullberg, "Channel capacity of Middleton's class A interference channel," *Electron. Lett.*, vol. 45, no. 24, pp. 1227–1229, Nov. 2009.

- [32] O. Hooijen, "A channel model for the residential power circuit used as a digital communications medium," *IEEE Trans. Electromagn. Compat.*, vol. 40, no. 4, pp. 331–336, Nov. 1998.
- [33] M. Loipez-Beniitez and F. Casadevall, "Versatile, accurate, and analytically tractable approximation for the Gaussian Q -function," *IEEE Trans. Commun.*, vol. 59, no. 4, pp. 917–922, Apr. 2011.
- [34] S. S. Gupta, "Probability integrals of multivariate normal and multivariate t_1 ," *Ann. Math. Stat.*, vol. 34, no. 3, pp. 792–828, Sep. 1963.
- [35] S. Boyd and L. Vandenberghe, *Convex Optimization*, 1st ed. New York: Cambridge University Press, 2004.